Catalytic Mechanism of *Escherichia coli* Alkaline Phosphatase: Resolution of Three Variants of the Acyl-Enzyme Mechanism†

Will Bloch* and Michael S. Gorby‡

ABSTRACT: Three variants of the classical acyl-enzyme mechanism were compared theoretically with respect to the predicted transient kinetics of substrate hydrolysis by *Escherichia coli* alkaline phosphatase. In all three, acyl-enzyme hydrolysis was assumed to be steady-state rate controlling, and the enzyme was assumed to exist initially primarily as a noncovalent complex with the acid product, inorganic phosphate. In one mechanism, the pre-steady-state rate-controlling step was assumed to be the dissociation of acid product from its initial complex with enzyme. In the other two, pre-steady-state rate control was assigned to an enzyme isomerization occurring before or after substrate binding to free enzyme. Under concentration conditions of excess substrate and acid product, integrated rate laws were used to reject the possibility of pre-steady-state rate control by enzyme isomerization between phosphate dissociation and substrate binding. Whereas this mechanism predicts a pre-steady-state noncompetitive relationship between substrate and acid product, the stopped-flow kinetics of 4-methylumbelliferyl phosphate hydrolysis demonstrates a competitive relationship, consistent with either of the other two mechanisms. Under concentration conditions of stoichiometrically limiting substrate, computer simulations eliminated the possibility of rate control by enzyme isomerization after substrate binding. This mechanism predicts a substrate concentration dependence for the apparent first-order rate constant of substrate hydrolysis which disagrees with previously published data [Halford, S. E. (1971) *Biochem. J. 125*, 319–327]; the other two mechanisms are consistent with experiment. Comparison of transient kinetic theory and experiment under these two contrasting concentration conditions suggests strongly that the rate-controlling step in phosphate ester hydrolysis by *E. coli* alkaline phosphate is the dissociation of "sticky" acid product from its noncovalent complex with enzyme. This mechanism explains an anomaly in the stopped-flow kinetic trace, a substoichiometric pre-steady-state burst of alcohol product release.

Alkaline phosphatase from *Escherichia coli* (EC 3.1.3.1) is a nonspecific phosphomonoesterase which is believed to obey an acyl-enzyme mechanism (Reid et al., 1969; Levine et al., 1969; Barrett et al., 1969) analogous to that observed for many carboxylic acid esterases and amidases. Scheme I presents this mechanism in its simplest form.[1] Spencer & Sturtevant (1959) showed that if the back reactions of steps 2–4 could be neglected and if step 1 was much faster than steps 2 and 3, the integrated rate law for the appearance of the alcohol product has the form of eq 1. Then the kinetic trace consists

$$[P]_t = \alpha t + \beta(1 - e^{-\gamma t}) \quad (1)$$

of a linear steady-state phase (rate = α) preceded by an exponential approach to the steady state (amplitude = β, first-order rate constant = γ) known as the pre-steady-state "burst".

When the reaction kinetics is studied by stopped-flow means, via the release of chromophoric or fluorescent alcohol product, step 2 reports on the reaction progress. A necessary condition for the appearance of burst kinetics is that the slowest (steady-state rate-controlling) fundamental process in the mechanism lie after the color-forming step. With alkaline phosphatase under acid conditions, a burst is observed because step 3 is steady-state rate controlling. However, k_3 varies directly with pH; it is too large to be steady-state rate controlling at pH values above 7 where no burst is observed (Aldridge et al., 1964; Fernley & Walker, 1966). The process

Scheme I

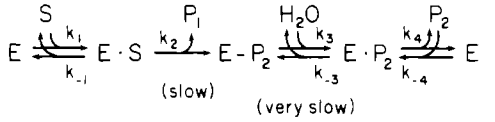

which limits the progress of the pre steady state at acid pH values is steady-state rate controlling under alkaline conditions (Halford et al., 1972). The rest of this paper will concentrate on interpretation of the burst parameters, β and γ, at an acid pH value where they are easily measurable, although any resulting microscopic insights must apply to the slowest step in the mechanism at pH values above 7.

As written, Scheme I cannot predict all of the details in the alkaline phosphatase kinetic literature. Contrary to the expectations of Spencer & Sturtevant (1959), step 2 cannot be pre-steady-state rate determining (Trentham & Gutfreund, 1968). As alternatives, it was proposed that pre-steady-state control resides in a relatively slow enzyme isomerization step after (Trentham & Gutfreund, 1968) or before (Reid & Wilson, 1971) substrate binding as shown in Schemes II and III, respectively. Transient (Reid & Wilson, 1971; Halford et al., 1969; Halford, 1971) and relaxation (Halford, 1972) kinetic data were obtained supporting each of these schemes or a combination of the two. Then it was shown that the native enzyme purified from *E. coli* is almost saturated with P_2 before it is reacted with substrate in the stopped flow (Bloch &

† From the Department of Chemistry, Reed College, Portland, Oregon 97202. *Received January 28, 1980.* The work was supported by the National Science Foundation under Grant No. PCM 78-07684.

* Correspondence should be addressed to this author at the Institute of Molecular Biology, University of Oregon, Eugene, OR 97403.

‡ Taken in part from the B.A. thesis of M.S.G., Reed College, 1978. Present address: University of Texas Health Science Center, Dallas, TX 75235.

[1] Abbreviations used: E, free enzyme; S, free substrate; E·S or E′·S, enzyme–substrate complex; P_1, alcohol product; P_2, acid product (inorganic phosphate in the case of alkaline phosphatase); E–P_2 or E′–P_2, acyl enzyme (phosphoryl enzyme in the case of alkaline phosphatase); E·P_2 or E′·P_2, noncovalent enzyme–acid product complex; E and E′ represent different isomeric forms of enzyme; Tes, 2-[[2-hydroxy-1,1-bis(hydroxymethyl)ethyl]amino]ethanesulfonic acid; DEAE, diethylaminoethyl; Tris, 2-amino-2-(hydroxymethyl)-1,3-propanediol.

0006-2960/80/0419-5008$01.00/0

Scheme II

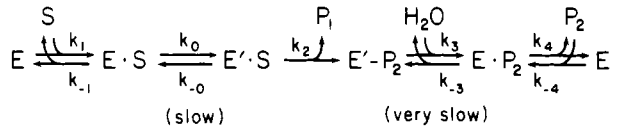

Scheme III

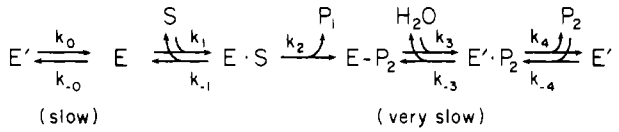

Schlesinger, 1973). Schemes II and III would still be relevant in such a case, provided that it is understood that the enzyme starts out in the $E{\cdot}P_2$ or $E'{\cdot}P_2$ state and provided that P_2 dissociation from this form is rapid on the time scale of the burst transient. However, an even simpler hypothesis for pre-steady-state rate control is that it occurs in the phosphate-dissociation step (Bloch & Schlesinger, 1973; Hull et al., 1976). In such a case Scheme I might be adequate to describe the catalytic mechanism, provided that it is understood that the enzyme starts out in the $E{\cdot}P_2$ state and provided that $k_2 \gg k_4$. Then no isomerization step would be required to explain the transient kinetic behavior of alkaline phosphatase.

Rate law derivations for the portions of Schemes I–III prior to step 2 (considering step 4 to be the first step when phosphate-containing or supplemented native enzyme is used) have suggested that the three mechanisms can be distinguished from one another simply on the basis of the substrate or phosphate concentration dependence of the γ parameter in eq 1 (Halford, 1971; Bloch & Schlesinger, 1973). These derivations were all based on the assumptions that during the pre-steady-state phase (a) step 1, step 2, and (except for Scheme I, where phosphate dissociation is burst rate limiting) step 4 are sufficiently faster than the burst that they are completely equilibrated on the burst time scale and (b) the reaction is kinetically controlled by the next to slowest process in the entire mechanism (step 4 in Scheme I and step 0 in Schemes II and III). Assumption a posited preequilibrium for steps 1, 2, and 4. Assumption b was based on the intuition that step 2 could have no direct influence on the ligand concentration dependence of the burst because it is so much faster (Trentham & Gutfreund, 1968) than the burst. The resulting burst rate constant expressions for concentration conditions of $[S]_0$, $[P_2]_0 \gg [E]_0$ predicted that γ should vary inversely with $[S]_0$ if Scheme I or III is correct and directly with $[S]_0$ if Scheme II is correct (Halford, 1971; Bloch & Schlesinger, 1973). They predicted that γ should vary directly with $[P_2]_0$ if Scheme I is correct and inversely with $[P_2]_0$ if Scheme II or III is correct (Bloch & Schlesinger, 1973).

There are two reasons why this body of theory is inappropriate for delineating the catalytic mechanism of alkaline phosphatase. (a) Step 2 appears to be so unidirectional that insufficient alcohol has accumulated during the burst to have equilibrated with enzyme–substrate complex and phosphoryl enzyme. (b) The rate constant expressions derived under conditions of excess substrate and product were used to interpret stopped-flow kinetic traces obtained with stoichiometrically limiting substrate (Halford, 1971). Rate law derivations depend so strongly on boundary-condition assumptions that one must not ignore limiting-reagent approximations in comparing theory and experiment. The work described here addresses these problems in two ways. (a) Integrated rate laws for Schemes I–III are derived without the assumption that step 2 has equilibrated and are used to interpret kinetic traces obtained under conditions of $[S]_0$, $[P_2]_0 \gg [E]_0$. They contradict some of the concentration-dependence predictions for γ made under the preequilibrium assumptions described above and permit discrimination of Scheme III from the other two mechanisms. (b) Digital computer simulations of Schemes I–III are performed under the concentration conditions of $[S]_0 \leq [E]_0 = [P_2]_0$, for which rate law derivation is impossible. They provide the first valid theoretical analysis of previously published stopped-flow data (Halford, 1971) and permit discrimination between Scheme II and the other two mechanisms.

Materials and Methods

Rate Law Derivation

Three integrated rate laws, one for each reaction scheme above, were derived and used to compute the substrate and acid-product concentration dependences of the pre-steady-state burst rate constant and amplitude for substrate hydrolysis (see paragraph at end of paper regarding supplementary material). The derivations involved application of integral calculus to differential rate laws, which, in turn, evolved from mass-action and material-balance equations. The rate laws and parameter expressions are generally applicable to any system obeying an acyl-enzyme mechanism. The computations depend on numerical estimates of the microscopic rate constants, based on published information about alkaline phosphatase from *E. coli*. In this section, we describe approximations needed to complete the derivations. The values assumed for the microscopic rate constants are documented in the subsequent description of kinetic stimulation.

Mechanistic Assumptions. For all three mechanisms, acyl-enzyme deacylation (step 3) is assumed to be much slower than all other steps, such that it is steady-state rate determining; and steps 1 and 2 are assumed to be much faster than other steps. For Scheme I, step 4 is assumed to be intermediate in rate, such that it might control approach to the steady state if the enzyme is present initially as a noncovalent complex with acid product. For Schemes II and III, step 4 is assumed to proceed at a rate similar to those of steps 1 and 2; and step 0 is assumed to be intermediate in rate, faster than step 3 and slower than steps 1, 2, and 4. In the presence of saturating acid product, the enzyme would start in the $E{\cdot}P_2$ or $E'{\cdot}P_2$ state for each mechanism as it would be observed in the stopped flow; step 2 should be assumed to be effectively unidirectional. Hence, the burst phase amounts to a redistribution of enzyme from $E{\cdot}P_2$ or $E'{\cdot}P_2$ to $E{-}P_2$ or $E'{-}P_2$, dominated kinetically by either step 4 (Scheme I) or step 0 (Schemes II and III). Because some of the intervening steps are much faster than the burst rate controlling process, they can be assumed to have equilibrated or reached a steady-state condition long before the reaction as a whole demonstrates steady-state behavior.

Exact solution of the differential equations for each mechanism requires that preequilibrium or steady-state relationships among the rapidly reacting intermediates be assumed to be valid. The latter are considered applicable to all intermediates consumed by a relatively rapid process: E in all three mechanisms, $E{\cdot}S$ in Schemes I and III, and $E'{\cdot}S$ in Scheme II. An intermediate consumed by a step equilibrating on the same time scale as the burst but generated by a much faster process should exist in approximate equilibrium with its immediate precursors during most of the burst phase, provided that the rate constant of the reverse reaction leading backward from the intermediate is larger than the burst rate constant. Hence, the preequilibrium approximation is probably more appropriate than the steady-state approximation for $E{\cdot}S$ in Scheme II and

E′ in Scheme III. However, in the interest of greatest generality, rate law derivation for these two mechanisms was done twice, once assuming preequilibrium and once assuming steady state for the intermediates just named.

Because alkaline phosphatase binds acid product very tightly (Reid et al., 1969; Bloch & Bickar, 1978), so tightly that the native enzyme is approximately saturated with acid product (Bloch & Schlesinger, 1973), this paper focuses on the transient kinetic behavior expected in the presence of associated acid product. However, in the interest of greatest generality, the rate law derivations were repeated for the three mechanisms under the condition that insufficient acid product is present to bind to enzyme even in the absence of competing substrate. These latter derivations were rendered quite simple by assuming that $[E{\cdot}P_2]$ or $[E'{\cdot}P_2]$ is much less than the concentration of any other enzyme species. There are two necessary conditions for the validity of this approximation, $k_3 \ll k_{-3}$ or k_4 and $[P_2] \ll (k_4 + k_{-3})/k_{-4}$. The first condition is met if deacylation is steady-state rate determining or if acyl-enzyme is more stable than the noncovalent enzyme–product complex. Both subconditions are obeyed by alkaline phosphatase at acid pH values, and the first one is commonly met by hydrolases showing pre-steady-state burst kinetics. The second necessary condition is met if acid product binds loosely to the enzyme. Although it does not apply in the case of alkaline phosphatase, it appears to be obeyed by most esterases and amidases.

Experimental

Reagents. Deionized, charcoal-treated, Gelman 0.2-μm filtered water (Continental Water Conditioning Corporation) was used for all solutions. Substrate was prepared by diluting a 3×10^{-3} M aqueous solution of 4-methylumbelliferyl phosphate (Sigma Chemical Co.), stored at 0 °C, into 0.10 M sodium acetate and 0.10 M NaCl, pH 5.18, immediately before reaction. Na_2HPO_4 solutions (10^{-1}–10^{-3} M) were diluted into the enzyme solution ~1 h before introduction into the stopped flow. The stopped-flow enzyme buffer was 0.010 M Tes (Sigma) and 0.10 M NaCl, pH 6.88. A 1:1 mixture of enzyme and substrate buffers had a pH of 5.28 at 20 °C. Reported substrate and phosphate concentrations, calculated from the masses dissolved during solution preparation, represent values in the stopped-flow cuvette.

The enzyme was isozyme 1 of alkaline phosphatase from *E. coli*, prepared and assayed as described previously (Bloch & Bickar, 1978) except in two respects: (a) protein was rechromatographed on DEAE-cellulose to remove isozyme 2; (b) catalytic activity was assayed in 0.10 M Tris-HCl, pH 8.0, instead of 1.0 M Tris-HCl, pH 8.0. The final enzyme concentration in the stopped-flow cuvette (2 active sites per molecule of molar mass 86 000) was calculated from the ultraviolet absorbance spectrum of a more concentrated protein solution ($E_{280,0.1\%}^{1cm} = 0.77$), together with the dilution factor used to prepare the enzyme for introduction into the stopped flow and the 1:2 dilution factor from mixing with substrate. This phosphatase preparation had a specific activity of 30 mol of *p*-nitrophenyl phosphate hydrolyzed per mol of enzyme molecules per s at 23 °C in 0.10 M Tris-HCl, pH 8.00.

Methods. A Durrum-Gibson stopped flow was used with a 1.54 cm light path fluorometer cuvette and a Schott KV 418 high-pass emission filter. Excitation was performed at 337.5 nm, the isosbestic point of 4-methylumbelliferone and its anion, with a 5-mm monochromator slit width and light from a 100-W tungsten–iodine bulb (Thorn Lighting) driven at 80 W under voltage regulation by a Sorensen SRL 40-6 power supply. The following stopped-flow parameters were used: 3 $\times 10^{-3}$ s dead time, 5×10^{-3} s photometer time constant, 700-V dynode potential, and 20 °C syringe bath and cuvette temperatures (the latter calibrated at 558 nm with 10^{-5} M phenol red in 0.1 M Tris-HCl, pH 8.0, and 0.05 M sodium pyrophosphate, pH 11.0). Kinetic traces (512 data points total) were collected at 0.02 or 0.05 V per division for 0.2–5.0 s in a Tektronix 7704A digital processing oscilloscope. After transfer to floppy-disk storage, traces were analyzed in a PDP 11/35 computer for nonlinear least-squares best fit to eq 1 by using a Basic language version of the CURFIT algorithm of Bevington (1969).

At least three (usually four) traces were analyzed for each combination of phosphate and substrate concentration; the error bars shown in Figures 4 and 5 represent the range of best-fit values obtained for a data point. The procedure used to collect each set of traces involved (1) measuring the base line signal by mixing substrate with enzyme buffer in the stopped flow, (2) calibrating the fluorescence signal by mixing substrate with a 7×10^{-5} M solution in enzyme buffer of 4-methylumbelliferone (Pfaltz & Bauer, recrystallized twice from methanol), and (3) recording traces while mixing substrate with enzyme. The difference between the first two voltages permitted calculation of the conversion factor needed to transform the best-fit amplitude and steady-state rate parameters from voltage to concentration units. Because of the inner filter effect generated by the significant absorbance of the more concentrated substrate solutions at 337.5 nm, this conversion factor increased in value 2.2-fold between 1.2×10^{-6} and 61×10^{-6} M substrate.

Kinetic Simulation

The time course of equilibration of each of the three reaction schemes discussed above was simulated digitally, starting with the concentrations of E, $E{\cdot}P_2$, P_2, and S expected when native alkaline phosphatase is mixed with substrate in a stopped-flow spectrophotometer. This section documents the initial concentrations assumed, the assumed values of the microscopic rate constants, and the simulation program and procedure.

Initial Conditions. The stoichiometric concentration of enzyme active sites was taken to be 1.9×10^{-5} M, twice the enzyme concentration value used in Halford's (1971) stopped-flow study. The initial stoichiometric concentration of inorganic phosphate was assumed to be equimolar with enzyme active sites; if this condition had not been met at least approximately in the previously published experiments, no first-order process slow enough to be followed in the stopped flow would have been observed (Bloch & Schlesinger, 1973). The initial concentration of substrate was varied from one simulation to the next, over most of the range reported by Halford (1971), 2×10^{-6} to 2×10^{-5} M.

The initial distribution of enzyme and phosphate over the species E or E′, $E{\cdot}P_2$ or $E'{\cdot}P_2$, and P_2 was calculated from assumed values of the equilibrium constant for step 4 and (in the case of Scheme III) for step 0. To assign these values, one must understand that although the stopped-flow reaction of enzyme and substrate is most commonly performed at pH 5.5, the native alkaline phosphatase (enzyme plus endogenous phosphate) is stored in dilute pH 8 or pH 7 buffer before mixing with substrate in more concentrated acidic buffer. Hence, the apparent dissociation constant for step 4 before mixing was assumed to be 2×10^{-6}, the value found experimentally at pH 8 (Bloch & Bicker, 1978). K_{eq} for step 0 in Scheme III at pH 8 was assumed to be 10^2 because phosphate-free enzyme shows an approximately site-stoichiometric instantaneous burst phase when mixed with substrate in the stopped flow. This fact implies that if Scheme III were obeyed,

the initial conformational equilibrium should favor E over E′ strongly.

Values for Microscopic Rate Constants. The values assumed for the microscopic rate constants must be tenuous because too few kinetic phases are observed to permit derivation of all microscopic parameters from the phenomenological ones, given the assumption that a particular mechanism is valid. Only order of magnitude accuracy of the estimates was sought, because the exercise was intended only to search for conspicuous differences among the schemes, not to simulate experimental results closely.

On the assumption that step 3 is steady-state rate limiting, k_3 could be estimated to be 0.5 s^{-1}, the steady-state rate constant at room temperature and pH 5.5 (Fernley & Walker, 1966; Bloch & Schlesinger, 1973). Both equilibrium (Reid et al., 1969) and kinetic (Levine et al., 1969) studies have yielded a value of 0.2 for k_3/k_{-3} near pH 5.5. Hence k_{-3} must be ~ 2.5 s^{-1}.

A value for k_2 has never been measured directly for oxyphosphate ester hydrolysis. However, a lower bound on the order of 10^3 s^{-1} can be estimated from the observation that stopped-flow reaction of substrate with phosphate-purged enzyme possesses an "instantaneous burst"; an active-site equivalent of substrate is hydrolyzed completely within the 3×10^{-3} s dead time of the stopped-flow spectrophotometer (Bloch & Schlesinger, 1973). All three mechanistic schemes predict that such purged enzyme should be in the E state when mixed with substrate. This observation that several half-times of the enzyme phosphorylation reaction have been completed within 3×10^{-3} s implies a phosphorylation half-time of 1×10^{-3} s or less, corresponding to a phosphorylation rate constant of 10^3 s^{-1} or greater.

For k_1 and k_{-1}, respective values of 2×10^9 M^{-1} s^{-1} and 10^2 s^{-1} have been estimated (Fernley & Walker, 1969). Although these values were inferred indirectly from marginal kinetic data by assuming a catalytic mechanism that is probably too simple, we use them here because they do not seem unreasonable; the value of k_1 is within the range usually attributed to diffusion control (Eigen & de Maeyer, 1963). Both equilibrium (Reid et al., 1969) and kinetic (Levine et al., 1969) investigations have suggested that the apparent dissociation constant for the noncovalent enzyme–phosphate complex is $\sim 1 \times 10^{-4}$ M near pH 5.5. For Schemes I and II, this variable would be equal to k_4/k_{-4}. For Scheme III, its value is influenced by the equilibrium constants for both step 4 and step 0, as shown in eq 2. For Scheme I, k_4 was assumed to be burst rate controlling and therefore to have a value near the burst rate constant of 20 s^{-1} (Fernley & Walker, 1966; Bloch & Schlesinger, 1973). Hence, k_{-4} was given an approximate value of 2×10^5 M^{-1} s^{-1} in tests of the kinetic consequences of Scheme I. For Schemes II and III, k_{-4} was assumed to be diffusion controlled and therefore to have a value near 5×10^8 M^{-1} s^{-1}. Hence, $k_4 = 5 \times 10^4$ s^{-1} for calculations of burst rate constants and amplitudes for Scheme II. For Scheme III, k_4 could be estimated from the measured value of K_{app} and the assumed value of k_{-4} only after a value for k_0/k_{-0} of 10^2 (see below) was assumed. Then $k_4/k_{-4} = 10^{-6}$ and $k_4 = 5 \times 10^2$ s^{-1}.

$$K_{app} = \frac{[P_2]([E] + [E'])}{[E'\cdot P_2]} = \frac{k_4}{k_{-4}}\left(1 + \frac{k_0}{k_{-0}}\right) \qquad (2)$$

For Schemes II and III, k_0 was assumed to be burst rate controlling and therefore to have a value near the burst rate constant of 20 s^{-1} (Fernley & Walker, 1966; Bloch & Schlesinger, 1973). There exists no direct estimate of k_{-0}, assuming either of these mechanisms to be valid. However, it has been inferred that the E′ state of Scheme II and the E state of Scheme III must have considerably higher affinities for substrate than the alternative conformations (E and E′, respectively) (Halford et al., 1969; Halford, 1971; Bloch & Schlesinger, 1973). In such a case k_0/k_{-0} must be significantly greater than 1. We have assumed that k_0/k_{-0} is ~ 100, so that k_{-0} has a value of ~ 0.2 s^{-1}.

Simulation Procedure. Simulations of Schemes I–III were performed on a PDP 11/70 time-shared computer with the NDTRAN interpreter, available from W. J. Davisson, Department of Economics, University of Notre Dame. The interval magnitude was set below the upper bound of values for which there was no significant variation of the computed transient rate constant (see below).

Transient rate constant and amplitude values were computed for each simulation from the kinetic trace for P_1 appearance, starting after 2×10^{-3} s of reaction (a lower-bound estimate of the stopped-flow dead time) and continuing for three half-lives of reaction. If the reaction was so fast that $t_{1/2}$ was less than 3.3×10^{-3} s, the trace was analyzed to 10^{-2} s. Because K_{eq} for substrate hydrolysis is very large and substrate was stoichiometrically limiting in every simulation, the trace was assumed to approach a final $[P_1]$ value of $[S]_0$ asymptotically, such that the trace could be linearized by plotting $\ln([S]_0 - [P_1]_t)$ vs. time. The transient rate constant was obtained from the slope of the unweighted linear least-squares best fit to this graph, even for the few traces which were conspicuously biphasic over the period analyzed, because the quality of the traces in the original experimental study (Halford, 1971) would not have permitted detection of biphasicity. The transient amplitude was taken to be the difference between $[S]_0$ and $[P_1]$ at 2×10^{-3} s. The instantaneous amplitude was observed as $[P_1]$ at 2×10^{-3} s, that portion of the reaction which would be complete in the stopped-flow dead time.

Results

Theoretical Expressions for Phenomenological Burst Parameters in the Presence of Excess Substrate and Acid Product. According to the rate law derivations (supplementary material), Schemes I–III have rate laws for P_1 appearance with the same form as eq 1, provided that [S] and $[P_2]$ are approximately constant over the observation period. The [S] and $[P_2]$ dependences of the two burst parameters are summarized in Table I. For each parameter, all three mechanisms yield algebraic expressions of similar form with one exception: the burst amplitude and rate constant expressions for Scheme III include $[S][P_2]$ cross-product terms in both numerator and denominator. These patterns suggest that at any single acid-product concentration, the substrate concentration dependence of either amplitude or rate constant would be insufficient to discriminate among mechanisms. However, the expressions lacking cross-product terms (Schemes I and II) predict a competitive relationship between S and P_2, whereas the expressions including cross-product terms (Scheme III) predict a noncompetitive relationship.

Table II summarizes the burst-parameter expressions for the three mechanisms in the absence of significant P_2 binding to the enzyme. For each parameter, the three mechanisms give identical functional dependences on [S], differing only in the exact combination of microscopic rate constants in the phenomenological expressions. It may also be shown that the expressions in Table I reduce exactly to those in Table II if $[P_2]$ is assumed to be zero valued. (For Scheme I, it is also necessary to assume that $k_4 \gg k_2$ and that $k_4 \gg k_{-3}$; although

Table I: Burst Rate Constant and Amplitude Expressions for Three Variants of the Acyl-Enzyme Mechanism[a]

reaction scheme	burst parameter
	Rate Constant Expression
I	$\dfrac{(k_4 + k_{-3})k_2k_1[S] + (k_2 + k_{-1})k_{-3}k_{-4}[P_2]}{(k_2 + k_{-1})k_4 + (k_2 + k_4)k_1[S] + (k_2 + k_{-1})k_{-4}[P_2]} + k_3$
II	$\dfrac{k_0k_4k_2k_1[S] + (k_{-0} + k_2)k_{-1}k_{-3}k_{-4}[P_2]}{k_4k_{-1}(k_{-0} + k_2) + (k_0 + k_{-0} + k_2)k_4k_1[S] + (k_{-0} + k_2)k_{-1}k_{-4}[P_2]} + k_3$
III	$\dfrac{k_2k_4k_0k_1[S] + (k_{-1} + k_2)k_{-0}k_{-3}k_{-4}[P_2] + k_{-3}k_2k_{-4}k_1[P_2][S]}{k_4(k_0 + k_{-0})(k_{-1} + k_2) + (k_0 + k_2)k_4k_1[S] + (k_{-1} + k_2)k_{-0}k_{-4}[P_2] + k_2k_{-4}k_1[P_2][S]} + k_3$
	Amplitude Expression
I	$\dfrac{\left((k_4 + k_{-3})k_2k_1[S] + (k_2 + k_{-1})k_{-3}k_{-4}[P_2]\right)k_4k_2k_1[S][E]_0}{\left((k_2 + k_{-1})k_3k_4 + \left[k_3(k_2 + k_4) + k_2(k_{-3} + k_4)\right]k_1[S] + (k_2 + k_{-1})(k_3 + k_{-3})k_{-4}[P_2]\right)^2}$
II	$\dfrac{\left((k_0k_4k_2k_1[S] + (k_{-0} + k_2)k_{-1}k_{-3}k_{-4}[P_2]\right)k_0k_4k_2k_1[S][E]_0}{\left(k_4k_3k_{-1}(k_{-0} + k_2) + \left[k_0(k_2 + k_3) + k_3(k_{-0} + k_2)\right]k_4k_1[S] + (k_3 + k_{-3})(k_{-0} + k_2)k_{-1}k_{-4}[P_2]\right)^2}$
III	$\dfrac{\left(k_2k_4k_0k_1[S] + (k_{-1} + k_2)k_{-0}k_{-3}k_{-4}[P_2] + k_{-3}k_2k_{-4}k_1[P_2][S]\right)k_4k_0k_2k_1[S][E]_0}{\left(k_3k_4(k_0 + k_{-0})(k_{-1} + k_2) + (k_2k_0 + k_3k_0 + k_3k_2)k_4k_1[S] + (k_{-1} + k_2)(k_3 + k_{-3})k_{-0}k_{-4}[P_2] + (k_3 + k_{-3})k_2k_{-4}k_1[P_2][S]\right)^2}$

[a] The reaction schemes and the definitions of the chemical components and microscopic rate constants are given in the introduction. The method of rate law derivation and the boundary conditions applied to intermediate concentrations are described under Materials and Methods. Apart from the assumption of preequilibrium for E·S in Scheme II and for E′ in Scheme III, steady-state behavior was assumed in all schemes for all intermediates between E·P_2 or E′·P_2 and E–P_2 or E′–P_2.

Table II: Burst Rate Constant and Amplitude Expressions for Three Variants of the Acyl-Enzyme Mechanism in the Absence of Significant Binding of P_2 to Enzyme[a]

reaction scheme	burst parameter
	Rate Constant Expression
I	$\dfrac{k_2k_1[S]}{(k_2 + k_{-1}) + k_1[S]} + k_3$
II	$\dfrac{k_0k_2k_1[S]}{k_{-1}(k_{-0} + k_2) + (k_0 + k_{-0} + k_2)k_1[S]} + k_3$
III	$\dfrac{k_0k_2k_1[S]}{(k_0 + k_{-0})(k_{-1} + k_2) + (k_0 + k_2)k_1[S]} + k_3$
	Amplitude Expression
I	$\left(\dfrac{k_2k_1[S]}{(k_2 + k_{-1})k_3 + (k_2 + k_3)k_1[S]}\right)^2[E]_0$
II	$\left(\dfrac{k_0k_2k_1[S]}{k_3k_{-1}(k_{-0} + k_2) + \left[k_0(k_2 + k_3) + k_3(k_{-0} + k_2)\right]k_1[S]}\right)^2[E]_0$
III	$\left(\dfrac{k_0k_2k_1[S]}{k_3(k_0 + k_{-0})(k_{-1} + k_2) + (k_2k_0 + k_3k_0 + k_3k_2)k_1[S]}\right)^2[E]_0$

[a] The only difference between the derivations used here and those leading to Table I is the assumption here that [E·P_2] or [E′·P_2] $\ll$ $[E]_0$ at all points on the kinetic trace. Apart from the assumption of preequilibrium for E·S in Scheme II, steady-state behavior was assumed in all schemes for all intermediates between E·P_2 or E′·P_2 and E–P_2 or E′–P_2.

these assumptions could not apply to alkaline phosphatase if it obeys Scheme I, they probably apply to any hydrolase with low affinity for acid product.)

Theroretical Values for Phenomenological Burst Parameters in the Presence of Excess Substrate and Acid Product. Figure 1 shows the computed substrate concentration dependences of the burst rate constant for Schemes I–III, given the microscopic rate constant values assigned under Materials and Methods. Figure 2 illustrates the corresponding graphs for the burst amplitude. For most values of [P_2], both burst parameters rise to saturation values as [S] is increased. However, the predicted competitive and noncompetitive interactions of S and P_2 are apparent. For Schemes I and II, the substrate concentration required to half-saturate the rate constant or burst amplitude increases with [P_2], but the saturation values of the parameters are [P_2] independent. For Scheme III, the half-saturation [S] values are [P_2] independent, but the saturation value of either parameter depends on [P_2].

The general utility of Figures 1 and 2 is limited by their dependence on specific rate constant values. Substrate-concentration dependences were computed for a range of k_{-3}

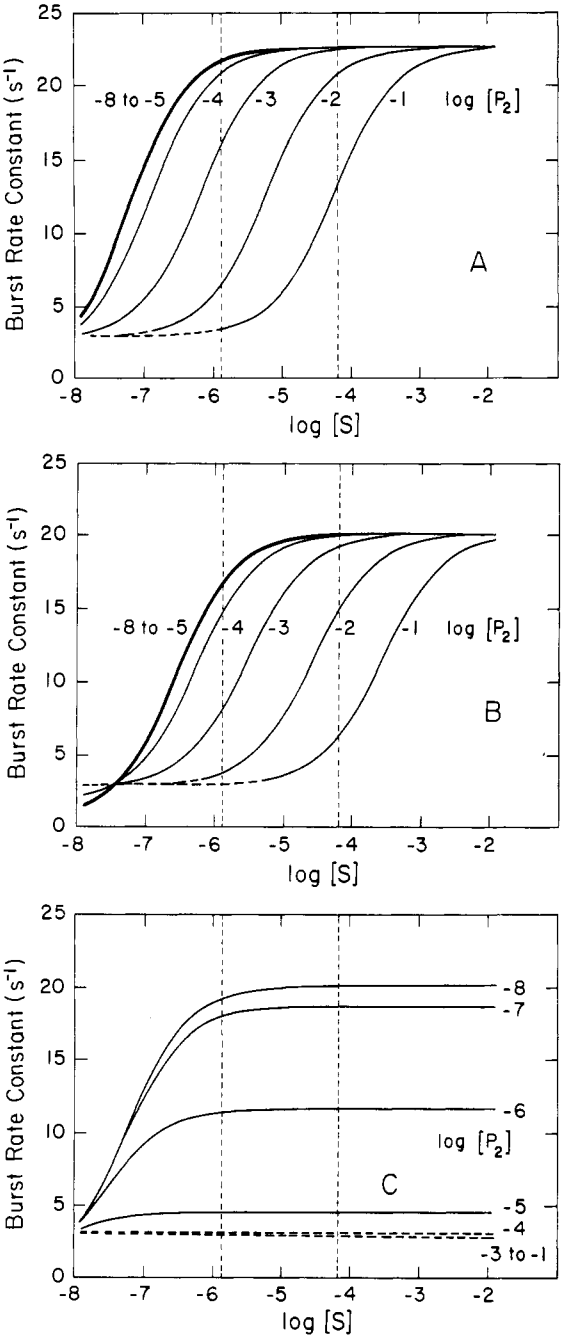

FIGURE 1: Substrate concentration dependences of the burst rate constant. A is based on Scheme I; B is based on Scheme II; C is based on Scheme III. The exact expressions used may be found in Table I. The assumed values of the microscopic rate constants are described under Materials and Methods. The dashed sections of the curves represent regions which might be experimentally inaccessible because the burst amplitude is <10% of the active-site concentration. The vertical dashed lines bound the substrate concentration range used in the experiments summarized in Figures 4 and 5. Concentrations are in units of molarity.

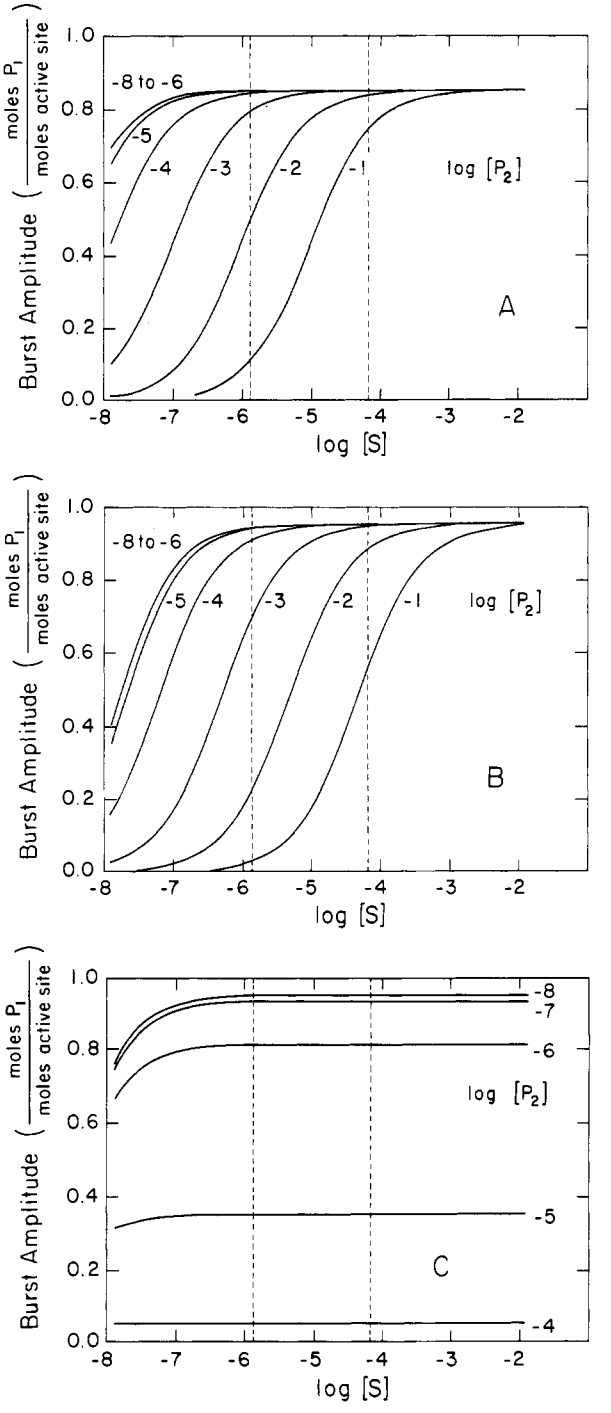

FIGURE 2: Substrate concentration dependences of the burst amplitude. A is based on Scheme I; B is based on Scheme II; C is based on Scheme III. The exact expressions used may be found in Table I. The microscopic rate constants used are the same as in Figure 1. The vertical dashed lines bound the substrate concentration range used in the experiments summarized in Figures 4 and 5.

values between 2.5 and 30 s^{-1} for each scheme, without changing the values of the other rate constants. For Scheme I, this perturbation had little effect on either competitive interaction between S and P_2. For Scheme II, the simple competitive pattern of the rate constant was destroyed as k_{-3} was increased, whereas the competitive pattern of the burst amplitude was unchanged. In the case of Scheme III, increasing k_{-3} had a radical effect on the [P_2] dependence of the substrate-saturated rate constant. At high k_{-3} values, this limiting value actually increased as [P_2] was increased, instead of decreasing in the manner of Figure 1C. However, the substrate-saturated burst amplitude experienced no such effect, retaining the general [P_2] dependence of Figure 2C. The qualitative insensitivity of the burst-amplitude patterns to the k_{-3} value suggests that this parameter may be the most useful in distinguishing among mechanisms.

Figure 2 permits one other comparison which is especially relevant to the phosphatase literature. The substrate-saturated burst amplitudes are significantly lower than the active-site stoichiometry: 15% lower for Scheme I and 5.5% lower for Schemes II and III. We studied this discrepancy as a function

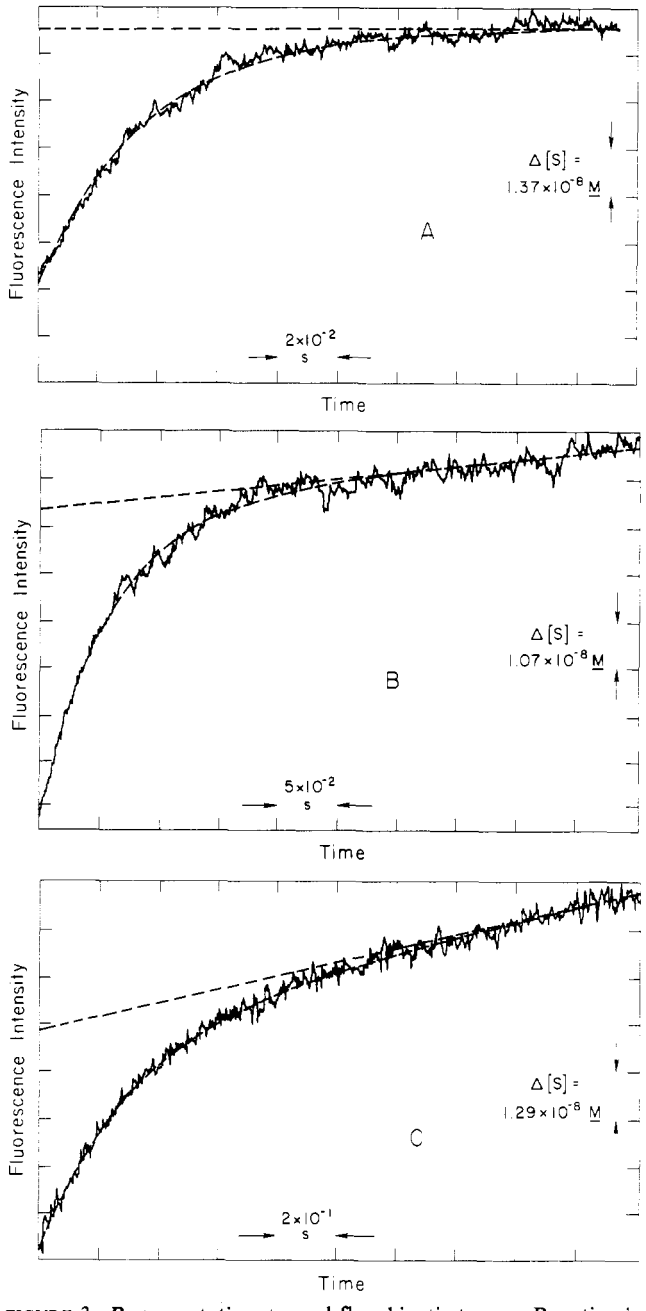

FIGURE 3: Representative stopped-flow kinetic traces. Reaction is the hydrolysis of 4-methylumbelliferyl phosphate by *E. coli* alkaline phosphatase at pH 5.28, 20 °C. $[E]_0 = 1.08 \times 10^{-7}$ M in sites; $[S]_0 = 4.4 \times 10^{-6}$ M. $[P]_0 = 8.0 \times 10^{-7}$ M in trace A, 4.0×10^{-5} M in trace B, 4.8×10^{-4} M in trace C. Dashed curve is least-squares best fit to eq 1. Dashed line is steady-state component of best fit.

of microscopic rate constant values. For all three mechanisms, amplitude approaches site concentration as k_3 is made progressively smaller than the forward rate constant of the burst rate-controlling step. An analogous trend was predicted for the classical acyl-enzyme mechanism (Spencer & Sturtevant, 1959), in which step 2 was assumed to be burst rate controlling and the burst amplitude at saturating S was shown to equal $[E]_0k_2^2/(k_2 + k_3)^2$. However, for Scheme I and only for Scheme I, the maximum burst amplitude also depends sharply on the k_4/k_{-3} ratio. Microscopically, it is clear that this effect is a short-circuiting of the normal pre-steady-state pathway. As k_{-3} approaches k_4 from below, an increasing fraction of $E{\cdot}P_2$ is transformed directly to $E{-}P_2$ without substrate hydrolysis; and the burst amplitude decreases from the site stoichiometry in a way that cannot be reversed by increasing

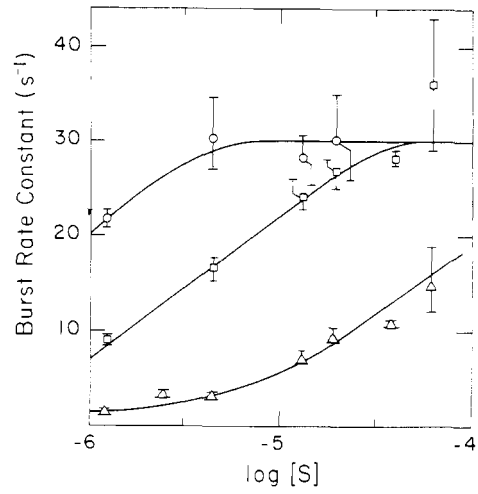

FIGURE 4: Dependence of burst rate constant on substrate and phosphate concentrations. Rate constant values are γ parameters from nonlinear least-squares best fit of stopped-flow kinetic traces to eq 1. Reactions were run as described under Materials and Methods. Phosphate concentrations were 8.0×10^{-7} (○), 4.0×10^{-5} (□), and 4.8×10^{-4} (△) M. Error bar indicates the range of values (at least three per data point).

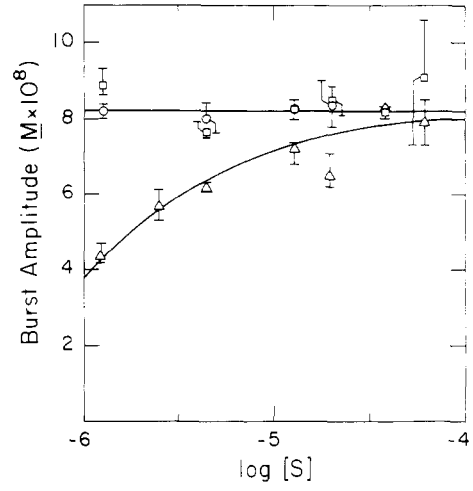

FIGURE 5: Dependence of burst amplitude on substrate and phosphate concentrations. Amplitude values are β parameters from nonlinear least-squares best fit of stopped-flow kinetic traces to eq 1. Reactions were run as described under Materials and Methods. Phosphate concentrations were 8.0×10^{-7} (○), 4.0×10^{-5} (□), and 4.8×10^{-4} (△) M. Error bar indicates the range of values (at least three per data point).

the k_4/k_3 ratio. Competition between the two processes consuming $E{\cdot}P_2$ is negligible in Schemes II and III, provided [S] is large enough and $[P_2]$ is small enough that $E{\cdot}P_2$ is completely and rapidly dissociated on the time scale of the burst.

Experimental Results for E. coli Alkaline Phosphatase in the Presence of Excess Substrate and Acid Product. Figure 3 shows representative stopped-flow kinetic traces for the phosphatase-catalyzed hydrolysis of 4-methylumbelliferyl phosphate at pH 5.3. Figures 4 and 5 summarize the experimental dependence of the pre-steady-state burst rate constant and amplitude on the substrate and phosphate concentrations. As predicted by Figures 1A,B and 2A,B, the burst amplitude at a given phosphate concentration was saturated at substrate concentrations lower than those required for the burst rate constant. For all three phosphate concentrations, the saturation value of the burst amplitude corresponded to 1.5 mol of P_i per mol of dimeric enzyme. For 4.8×10^{-4} M phosphate, the burst amplitude approached saturation over

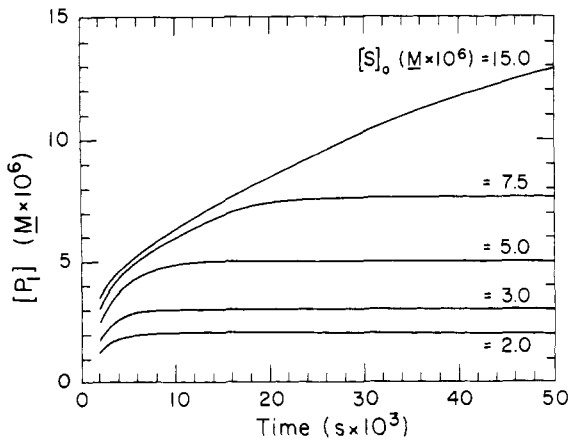

FIGURE 6: Simulated kinetic traces for Scheme I (rate control by acid-product dissociation). Graphs show predicted time course of alcohol-product appearance upon 1:1 stopped-flow mixing of native alkaline phosphatase (1.9×10^{-5} M in active sites) and any phosphomonoester (initial concentrations indicated next to traces) at pH 5.5, 20 °C.

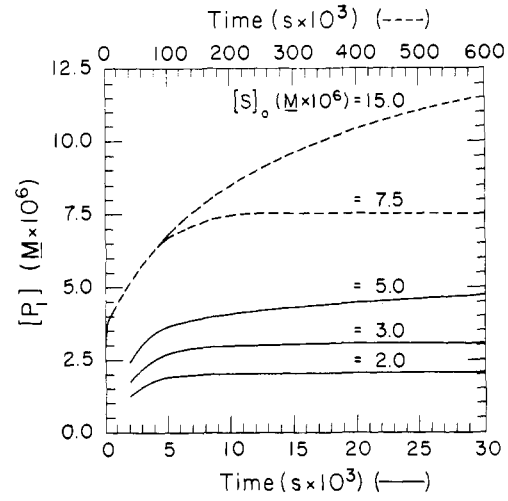

FIGURE 7: Simulated kinetic traces for Scheme III (rate control by enzyme isomerization prior to substrate binding). Graphs show predicted time course of alcohol-product appearance upon 1:1 stopped-flow mixing of native alkaline phosphatase (1.9×10^{-5} M in active sites) and any phosphomonoester (initial concentrations indicated next to traces) at pH 5.5, 20 °C.

the substrate concentration range of 1.2×10^{-6}–6.1×10^{-5} M, whereas for the lower phosphate concentrations, saturation was observed at all substrate concentrations. This comparison suggests that the saturating substrate concentration range is phosphate concentration dependent in accord with a competitive interaction of substrate and phosphate and in disharmony with a noncompetitive interaction. The burst rate constant data support the preceding conclusions. Although substrate saturation was not attained for the highest phosphate concentration, it is clear that as the phosphate concentration is increased, the substrate concentration range for saturation of the rate constant also is increased.

Simulated Kinetic Traces in the Presence of Limiting Substrate. Figures 6 and 7 show simulated kinetic traces for selected substrate concentrations for Schemes I and III, respectively. In both cases, close examination of the traces, especially at the higher substrate concentrations, suggests that two different processes control the observed transients. At low substrate concentration, a very fast process, with a rate constant near 10^3 s^{-1}, completely determines the trace. At $[S]_0$ above 3×10^{-6} M, a much slower phase is added to the trace.

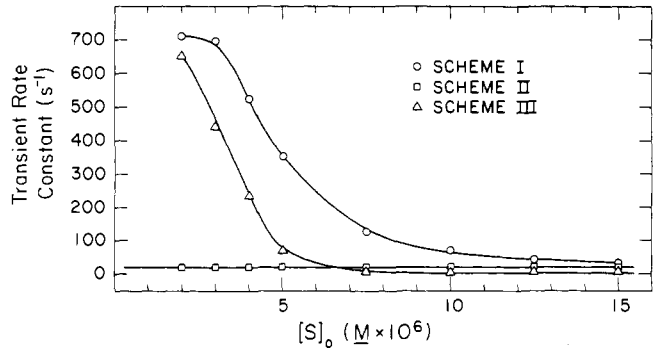

FIGURE 8: Substrate concentration dependence of apparent transient rate constant. Rate constant value was calculated from least-squares best-fit slope of log plot of simulated kinetic trace for all times beyond 2×10^{-3} s, the approximate stopped-flow dead time.

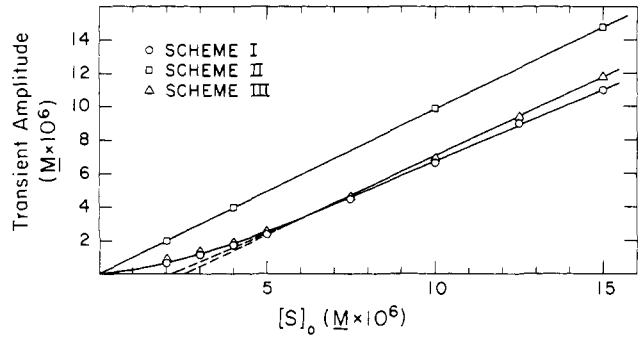

FIGURE 9: Substrate concentration dependence of transient amplitude. Amplitude was calculated as the difference between the infinite-time and 2×10^{-3} s values of $[P_i]$ for each simulated kinetic trace.

As $[S]_0$ is increased above 3×10^{-6} M, the amplitude of this slower component increases until it dominates the portion of the trace, at times greater than 2×10^{-3} s, which would be seen in the stopped flow. The faster process then is seen primarily as an instantaneous phase of substrate hydrolysis. Hence, the observed transient appears to become slower as the substrate concentration is increased, when what really is happening is the increased contribution of a slower process to a biphasic transient. Log plots of the traces (not shown) support this interpretation. For substrate concentrations above 5×10^{-6} M, even those plots which appear linear at times greater than 2×10^{-3} s become quite biphasic if extended back to zero time. In contrast, log plots for 2×10^{-6} and 3×10^{-6} M substrate are linear at all times.

The kinetic traces for Scheme II (not shown) were rigorously first order at all substrate concentrations. They gave a phenomenological rate constant value near 20 s^{-1}, the value assumed for k_0, regardless of substrate concentration. Scheme II generated no distinct instantaneous phase at any substrate concentration.

Figures 8 and 9 summarize the transient rate constant and amplitude results for all three mechanisms and all substrate concentrations examined. Whereas the apparent rate constants from Schemes I and III decrease by several orders of magnitude as substrate concentration is increased toward a value stoichiometric with enzyme active sites, the Scheme II rate constant is essentially unchanged. The substrate concentration dependence of the transient amplitude reinforces the distinction between Scheme II, on the one hand, and Schemes I and III, on the other. The Scheme II amplitude is equimolar with stoichiometric substrate concentration (representing a stoichiometric titration of enzyme active sites with substrate), because no sites can undergo the rate-controlling transition until they are occupied by substrate. The graphs of Scheme

I and III amplitudes vs. $[S]_0$ have a unitary slope only at $[S]_0 \geq 5 \times 10^{-6}$ M, being concave upward at lower concentrations. The linear portions of these graphs extrapolate to a zero transient amplitude at $[S]_0$ near 3×10^{-6} M. This value is close to the zero-time value of [E] in Schemes I and III, 3.9×10^{-6} M. In these mechanisms, those enzyme active sites which lie downstream from the rate-determining process at the time of mixing undergo very rapid reaction with substrate, leaving no substrate to react with sites which first must undergo this process, unless the total substrate concentration exceeds the concentration of rapidly reacting sites. At higher substrate concentrations, the substrate remaining after depletion of rapidly reacting sites is hydrolyzed as rapidly as the remaining sites undergo the rate-determining process.

Discussion

Revised Interpretation of Alkaline Phosphatase Transient Kinetics. The introduction to this paper suggested two weaknesses in previous theoretical analyses (Halford, 1971; Bloch & Schlesinger, 1973) of the transient kinetics of substrate hydrolysis by *E. coli* alkaline phosphatase: treatment of the catalytic burst as an approach to equilibrium rather than as an approach to a steady state and failure to respect limiting-reagent assumptions in comparing theory and experiment. The present rate law derivations and simulations verify the seriousness of the earlier errors.

Contrary to approach to equilibrium rate law predictions, Tables I and II and Figure 1 show that regardless of the mechanism, the burst rate constant obtained with excess substrate and acid product is expected to vary directly with $[S]_0$ and inversely with $[P_2]_0$, showing saturation behavior over some concentration range of each ligand. Hence, the previous claims that Scheme II could be distinguished by the $[S]_0$ dependence of γ and that Scheme I could be distinguished by the $[P_2]_0$ dependence of γ are untrue. The previously published rate constant expressions (Halford, 1971; Bloch & Schlesinger, 1973) may be adequate for the stopped-flow reaction of phosphatase with a substrate analogue which binds but does not react further (Halford et al., 1969; Halford, 1972); but they do not illuminate a catalytic sequence which includes a rapid unidirectional process, like step 2 in Schemes I–III. Instead, Table I and Figures 1 and 2 show that in the presence of excess substrate and acid product, Scheme III can be distinguished from the other two mechanisms on the basis of a noncompetitive, as opposed to competitive, inhibitory interaction between substrate and acid product.

The formalism of integrated rate laws is not necessary to explain the distinction among these mechanisms with respect to pre-steady-state inhibition patterns. In the first two, S and P_2 bind in a mutually exclusive manner to the same intermediate, E. In Scheme III, the two association reactions are separated by a process, step 0, which progresses on the pre-steady-state time scale being studied. Steady-state kinetics would not permit such a mechanistic distinction, showing a competitive interaction between S and P_2 for all three schemes, because step 0 equilibrates more rapidly than the steady-state rate-controlling process.

The earlier theoretical treatments of phosphatase transient kinetics (Halford, 1971; Bloch & Schlesinger, 1973) implied that the transient observed when $[S]_0 \leq [E]_0$ would be a single exponential process; the concentration dependences of its rate constant would be those predicted by rate laws derived for the concentration condition of $[S]_0$, $[P_2]_0 \gg [E]_0$. They concluded that the rate constant should vary inversely with $[S]_0$ if Scheme I or III were valid and directly with $[S]_0$ if Scheme III pertained, showing saturation behavior in either case. The present simulations contradict the previous prediction for Scheme II; Scheme II would produce a substrate concentration independent transient under the concentration conditions used experimentally (Halford, 1971). Figure 8 confirms the earlier predictions for Schemes I and III, but Figures 6, 7, and 9 show that this behavior arises for an unanticipated reason. The effect of increasing $[S]_0$ would be not to decelerate an isomerization or phosphate dissociation, but to transfer apparent rate control from a faster process to a slower one.

The slower processes are those anticipated for the two mechanisms: phosphate dissociation for Scheme II and enzyme isomerization for Scheme III. The fact that the phenomenological rate constant generated by Scheme III at high $[S]_0$ is an order of magnitude lower than k_0 can be attributed to the inhibitory effect of phosphate; substrate cannot competitively reverse this effect because phosphate binding and substrate binding are isolated from one another by the rate-controlling process. The faster process must lie between the rate-controlling process and step 2, the color-forming process; it is either substrate binding or step 2 itself. Although we have not attempted to show which is the case, the two possibilities should be distinguishable by observing the effect of varying k_1 and k_2 on the simulation transient rate constant at low substrate concentrations.

The simulations show that for Schemes I and III, the observed stopped-flow transient reports on the rapid reaction of E at low $[S]_0$ and on the much slower reaction of $E{\cdot}P_2$ or E′ at high $[S]_0$. This perception suggests that the quantitative details of the substrate concentration dependences of the transient amplitude and rate constant should be highly sensitive to the premixing solvent in which the enzyme is incubated. Addition of phosphate to the enzyme before reaction with substrate should serve to shift the concentration-dependence graphs to the left by diminishing the amount of rapidly reacting enzyme present to consume substrate before the slower process would be observed. The preincubated high-phosphate limiting behavior of Schemes I and III should resemble that of Scheme II shown here. Lowering the affinity of enzyme for phosphate would shift the concentration-dependence graphs to the right, toward higher substrate concentrations. Halford's kinetic data (1971) may well show such an effect on the rate constant upon shifting from 0.1 to 1.1 ionic strength; this change should increase the dissociation constant for phosphate at pH 8 (the premixing pH of the enzyme buffer) two- to threefold (Bloch & Bickar, 1978).

Catalytic Mechanism of Alkaline Phosphatase. This study has been directed toward the microscopic identification of that elementary process which controls the rate of the pre-steady-state burst of P_1 release observed when alkaline phosphatase is mixed with excess substrate at acid pH values. There is strong evidence that this selfsame process is steady-state rate controlling at pH values above 7 (Fernley & Walker, 1966; Halford et al., 1972) and therefore limits the efficiency of phosphatase catalysis under physiological conditions. The simulations, summarized in Figure 8, show clearly that this process cannot be an enzyme isomerization following substrate binding. Comparison of the simulated and experimentally observed (Halford, 1971) reaction kinetics under conditions of stoichiometrically limiting substrate permits pre-steady-state rate control to be assigned either to phosphate dissociation from a noncovalent complex with enzyme or to an enzyme isomerization between phosphate dissociation and substrate binding. However, theoretical and experimental studies under concentration conditions of excess substrate and acid product (Figures 1–5) eliminate the latter mechanism from further

consideration. Hence, of the three mechanisms being compared, only the simplest one, Scheme I, is consistent with the detailed concentration dependences seen when substrate hydrolysis is studied in the stopped flow under two different concentration conditions. At pH values above 7 (Fernley & Walker, 1966), phosphatase must be kinetically limited in the steady state by the rate of dissociation of tightly and noncovalently bound product. In this regard, it resembles a number of dehydrogenases (Raval & Wolfe, 1962; Silverstein & Sulebele, 1969; Heck, 1969; DiFranco & Iwatsubo, 1971; Shore & Gutfreund, 1970; Czeisler & Hollis, 1973; DeTraglia et al., 1977). Several kinases may also observe this behavior (Nageswara Rao et al., 1976, 1978a,b, 1979).

Hull et al. (1976) originally proposed that phosphate dissociation should be steady-state rate controlling at pH 8 (and hence, pre-steady-state rate controlling at acid pH values), from ^{31}P NMR line width studies of equilibrium mixtures of enzyme and inorganic phosphate. They showed that the rate constant for phosphate dissociation or an enzyme isomerization prior to phosphate dissociation was low enough to account for the catalytic turnover number seen under nonequilibrium conditions. The present work complements and extends that conclusion in three ways: (a) operation at acid pH values, (b) operation far from equilibrium, and (c) logical elimination of hypothesized mechanistic alternatives. However, we have not attempted to resolve the two reaction models proposed by Hull et al. (1976); theoretical and experimental tests of this question are currently under way in this laboratory. Nothing described here suggests the involvement of any sort of conformational change in catalysis by *E. coli* alkaline phosphatase.

In addition to delineating the simplest sequence of fundamental processes needed to describe the phosphatase catalytic mechanism and to showing which of these must be rate limiting, the results presented here appear to solve a longstanding mystery in the stopped-flow study of alkaline phosphatase. The phosphatase molecule is composed of two identical or nearly identical polypeptide subunits (Rothman & Byrne, 1963; Knox & Wyckoff, 1973). Classically it was observed that the burst transient had an amplitude corresponding to one substrate molecule hydrolyzed per enzyme dimer (Fernley & Walker, 1966; Ko & Kezdy, 1967; Trentham & Gutfreund, 1968; Halford, 1971), even when enzyme was saturated with substrate and the burst amplitude was corrected for the effect of incomplete steady-state rate control by phosphoryl enzyme deacylation (Spencer & Sturtevant, 1959). These results led to the hypothesis that the enzyme possessed anticooperative site interactions (Halford et al., 1969; Halford, 1971; Lazdunski et al., 1971). Later, it was shown that failure to saturate the enzyme with inorganic phosphate before reaction with substrate resulted in a variable and diminished transient amplitude (Bloch & Schleisnger, 1973). However, even with saturating phosphate before mixing and saturating substrate after mixing, the maximum observed burst amplitude was only 1.5–1.6 mol of substrate hydrolyzed per mol of enzyme dimer (Bloch & Schlesinger, 1973, 1974). Our use here of rate laws to examine the sensitivity of burst amplitude to the magnitudes of k_3, k_{-3}, and k_4 shows that such behavior is expected for Scheme I and only for Scheme I among those mechanisms tested. The microscopic origin of the phenomenon is clear. The 0.4 mol of substrate per mol of enzyme dimer which is not hydrolyzed before the onset of the steady state represents those phosphate-occupied enzyme active sites which proceed to the steady-state rate-limiting species via a non-color-forming shortcut, direct phosphorylation of enzyme by noncovalently bound phosphate. The significance of this pathway depends totally on the relative magnitudes of k_{-3} and k_4 in Scheme I. Given that at pH 5.5, 20 °C, k_4 must approximate 20 s^{-1} to account for the observed transient rate constant under these conditions, k_{-3} must approximate 5 s^{-1} to cause a 20% depeletion of $E{\cdot}P_2$ through direct enzyme phosphorylation. This value agrees adequately with the value of 2.5 s^{-1} used in the simulations and estimated with the help of equilibrium considerations (see Materials and Methods).

Relationship of This Work to Enzyme Mechanistic Studies in General. The theoretical results described here have implications extending far beyond the mechanism of alkaline phosphatase. Rate laws were derived in such a general manner that the results in Tables I and II might be applicable to many enzymes possessing a covalent enzyme–product catalytic intermediate, provided that the microscopic rate constants obey the same inequality relationships assumed here. Although the especially strong binding of acid product to enzyme in the case of alkaline phosphatase has caused us to focus on the rate laws which apply when such binding is significant, we have also developed the rate laws which pertain to hydrolases which do not bind product tightly. These expressions make it clear that Schemes I–III cannot be distinguished via the transient kinetic study of substrate hydrolysis when $[S]_0 \gg [E]_0$ unless a competitive or noncompetitive interaction of acid product with substrate can be demonstrated.

There is one way in which the present rate laws have limited generality. We have restricted attention to sets of microscopic rate constants and initial concentrations which would generate a kinetic trace for P_i consisting of a negative exponential burst phase leading into a linear steady-state phase. Our results do not illuminate experimental systems in which the burst or steady state is preceded by a lag phase. A more general treatment which might be adapted to Scheme I without any explicit limitations on the relative magnitudes of microscopic rate constants has been given by Hijazi & Laidler (1973).

The present work suggests several general methodological conclusions regarding the transient kinetic study of the enzyme catalytic mechanism. (a) Rate law derivation depends critically on the conditions of unidirectionality and bidirectionality which are assumed. (b) An elementary process which is not rate controlling may nevertheless influence the concentration dependences of the observed transient parameters, merely through its thermodynamic pull on a rate-determining process. (c) Pre-steady-state kinetic parameters may reveal competitive or noncompetitive interactions between product and substrate which differ from those predicted for steady-state parameters and which, like steady-state inhibition patterns, help to distinguish mechanistic alternatives. (d) The burst amplitude may be more useful than the burst rate constant in discriminating among hypothetical reaction schemes, because its concentration dependence is less sensitive to the relative magnitudes of the microscopic rate constants. (e) Use of the substrate-saturated burst amplitude to count active sites may give artifactually low answers in the presence of a sticky product which can short-circuit the catalytic path to the principal steady-state intermediate. (f) The mechanistic resolving power of a transient study may depend on whether enzyme or substrate is stoichiometrically limiting. Hence, the results obtained under these two conditions may be complementary. (g) Accordingly, kinetic-trace simulation and rate law derivation represent complementary, rather than alternative, theoretical methods.

Acknowledgments

We are grateful to Graham Ross for help in digital computation and to Russell Tonkyn for first questioning the ap-

proach to equilibrium treatment of pre-steady-state substrate hydrolysis.

Supplementary Material Available

Derivations of integrated rate laws for Schemes I–III (11 pages). Ordering information is given on any current masthead page.

References

Aldridge, W. N., Barman, T. E., & Gutfreund, H. (1964) *Biochem. J. 92*, 23c–25c.

Barrett, H. W., Butler, R., & Wilson, I. B. (1969) *Biochemistry 8*, 1042–1047.

Bevington, P. R. (1969) *Data Reduction and Error Analysis for the Physical Sciences*, pp 235–242, McGraw-Hill, New York.

Bloch, W., & Schlesinger, M. J. (1973) *J. Biol. Chem. 248*, 5794–5805.

Bloch, W., & Schlesinger, M. J. (1974) *J. Biol. Chem. 249*, 1760–1768.

Bloch, W., & Bickar, D. (1978) *J. Biol. Chem. 253*, 6211–6217.

Czeisler, J. L., & Hollis, D. P. (1973) *Biochemistry 12*, 1683–1689.

DeTraglia, M. C., Schmidt, J., Dunn, M. F., & McFarland, J. T. (1977) *J. Biol. Chem. 252*, 3493–3500.

DiFranco, A., & Iwatsubo, M. (1971) *Biochimie 53*, 153–159.

Eigen, M., & de Maeyer, L. C. (1963) *Tech. Org. Chem. 8 (Part 2)*, 1031–1050.

Fernley, H. N., & Walker, P. G. (1966) *Nature (London) 212*, 1435–1437.

Fernley, H. N., & Walker, P. G. (1969) *Biochem. J. 111*, 187–194.

Halford, S. E. (1971) *Biochem. J. 125*, 319–327.

Halford, S. E. (1972) *Biochem. J. 126*, 727–738.

Halford, S. E., Bennett, N. G., Trentham, D. R., & Gutfreund, H. (1969) *Biochem. J. 114*, 243–251.

Halford, S. E., Lennette, D. A., & Schlesinger, M. J. (1972) *J. Biol. Chem. 247*, 2095–2101.

Heck, H. d'A. (1969) *J. Biol. Chem. 244*, 4375–4381.

Hijazi, N. H., & Laidler, K. J. (1973) *Can. J. Biochem. 51*, 822–831.

Hull, W. E., Halford, S. E., Gutfreund, H., & Sykes, B. D. (1976) *Biochemistry 15*, 1547–1561.

Knox, J. A., & Wyckoff, H. W. (1973) *J. Mol. Biol. 74*, 533–545.

Ko, S. H. D., & Kezdy, F. J. (1967) *J. Am. Chem. Soc. 89*, 7139–7140.

Lazdunski, M., Petitclerc, C., Chappelet, D., & Lazdunski, C. (1971) *Eur. J. Biochem. 20*, 124–139.

Levine, D., Reid, T. W., & Wilson, I. B. (1969) *Biochemistry 8*, 2374–2380.

Nageswara Rao, B. D., Buttlaire, D. H., & Cohn, M. (1976) *J. Biol. Chem. 251*, 6981–6986.

Nageswara Rao, B. D., Cohn, M., & Nada, L. (1978a) *J. Biol. Chem. 253*, 1149–1158.

Nageswara Rao, B. D., Cohn, M., & Scopes, R. K. (1978b) *J. Biol. Chem. 253*, 8056–8060.

Nageswara Rao, B. D., Kayne, F. J., & Cohn, M. (1979) *J. Biol. Chem. 254*, 2689–2696.

Raval, D., & Wolfe, R. G. (1962) *Biochemistry 1*, 1112–1117.

Reid, T. W., & Wilson, I. B. (1971) *Biochemistry 10*, 380–387.

Reid, T. W., Pavlic, M., Sullivan, D., & Wilson, I. B. (1969) *Biochemistry 8*, 3184–3188.

Rothman, F., & Byrne, R. (1963) *J. Mol. Biol. 6*, 330–340.

Shore, J. D., & Gutfreund, H. (1970) *Biochemistry 9*, 4655–4659.

Silverstein, E., & Sulebele, G. (1969) *Biochemistry 8*, 2543–2550.

Spencer, T., & Sturtevant, J. M. (1959) *J. Am. Chem. Soc. 81*, 1874–1882.

Trentham, D. R., & Gutfreund, H. (1968) *Biochem. J. 106*, 455–460.

Micrococcus luteus Endonucleases for Apurinic/Apyrimidinic Sites in Deoxyribonucleic Acid. 1. Purification and General Properties†

Josiane Pierre and Jacques Laval*

ABSTRACT: Two chromatographically distinct endonucleases from *Micrococcus luteus*, specific for apurinic and apyrimidinic sites (AP-endonucleases A and B), have been extensively purified and characterized. Both are free from DNA glycosylase, unspecific endonuclease, and phosphatase activities. The two enzymes behave as monomeric proteins of ~35 000 daltons. In addition to their different chromatographic properties on CM-cellulose, P-cellulose, hydroxylapatite, and DNA–Sepharose, both AP-endonucleases can be distinguished as follows: AP-endonuclease A has an isoelectric point of 4.8, shows a half-life of 4 min at 45 °C, reacts optimally at pH 7.5 and has a K_M value of 2.3×10^{-6} M. AP-endonuclease B has a p*I* of 8.8, is more stable at 45 °C (half-life of 10 min), and reacts optimally between pH 6.5 and pH 8.5; its K_M value is 3.7×10^{-6} M.

Apurinic sites (AP sites)[1] are generated in the DNA of living cells through different pathways. They are due to spontaneous hydrolysis of purine glycosyl bonds, which occurs at a nonnegligible rate even at neutral pH (Greer & Zamenhof, 1962). They also occur through chemical depurination of alkylated bases (Margison & O'Connor, 1973). Furthermore, some alkylated or damaged bases are enzy-

† From LA 147 CNRS and U140 INSERM, Institut Gustave-Roussy, 94800 Villejuif, France. *Received March 7, 1980.* This work was supported by CNRS, CRL-INSERM, and CEA grants and by a fellowship (to J.P.) of the Ligue Nationale Française contre le Cancer.

[1] Abbreviations used: Hepes, *N*-2-hydroxyethylpiperazine-*N'*-2-ethanesulfonic acid; SSC, 0.15 M NaCl and 0.015 M sodium citrate, pH 7.0; EtdBr, ethidium bromide; AP site, apurinic/apyrimidinic site; NaDodSO$_4$, sodium dodecyl sulfate.

0006-2960/80/0419-5018$01.00/0